RF PARAMETERS OF A TE - TYPE DEFLECTING STRUCTURE FOR THE S-BAND FREQUENCY RANGE *

V. Paramonov [†], L. Kravchuk, INR RAS, Moscow, Russia

K. Floettmann, DESY, Hamburg, Germany

Abstract

In [1]an effective compact deflecting structure has been proposed preferably for the L-band frequency range. RF parameters of this structure are now considered for S-band frequencies both for traveling and standing wave operation. Some methodical topics of the structure are discussed too.

INTRODUCTION

In [1] a deflecting structure was proposed with the original design idea to separate the functions of RF efficiency and RF coupling, which are coupled in the well known Disk Loaded Waveguide (DLW) by a single parameter - the aperture radius r_a. Two protrusions are introduces at the disk in order to concentrate the transverse electric field at the axis, Fig.1b. The magnetic field around the protrusions, Fig. 1d, provides the required flux for the transverse RF voltage. The structure has a small transverse diameter $2r_c \sim (0.6 \div 0.8)\lambda_0$, where λ_0 is the operating wavelength and looks promising at lower frequencies, including the L-band range. The structure dispersion is positive with a passband width $\Delta f \sim (0.10 \div 0.15)f_0$. It reaches a significant group velocity β_g for a Traveling Wave (TW) with a phase advance $0 < \theta < \pi$, which results in a significant power flow and thus suggest a Standing Wave (SW) operation, [2].
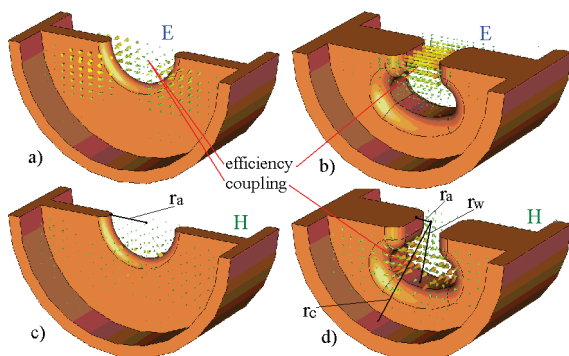
Figure 1: Electric (a, b) and magnetic (c, d) field distributions for the classical DLW structure (a, c) and the TE-deflector, (b, d).

The attractive features of the structure stimulate an additional study, including possible applications in the S - band frequency range.

FIELD DISTRIBUTION

The classification of a structure with a complicated field distribution is always rather conditional. In the field distributions, Fig. 1b,d, one can see a strong transverse electric field, providing an argument for a structure classification in the RF sense as TE - type. But for the description of a deflecting field at $\beta = 1$ the generating hybrid waves HM_n and HE_n are used, see [3] for explanations, both with simultaneously non vanishing E_z and H_z components. For the deflecting force - the transverse component of the Lorenz force - in cylindrical or Cartesian coordinates we have:

$$\vec{F}_{r,x}^L = e(\vec{E} + [\vec{v}, \vec{B}]) = e(E_r - \beta Z_0 H_\varphi) = \quad (1)$$
$$= e(E_x - \beta Z_0 H_y), \quad Z_0 = \sqrt{\mu_0 \epsilon_0}.$$

In contrast to a DLW, the structure under consideration has the same phasing for both transverse components E_r, H_φ or E_x, H_y and the deflecting effect of the electric field is partially compensated by an opposite deflection of the magnetic field. The phasing of transverse E, H components defines also the sign of the group velocity, which is positive in our case. For a deflection of particles this structure can be described as HE_1-dominating structure.

The effective transverse shunt impedance Z_e in the structure,

$$Z_e = \frac{|\frac{1}{k} \int_0^L \frac{\partial E_z}{\partial z} e^{ikz} dz|^2}{P_s L}, \quad \beta = 1, \quad (2)$$

where L is the structure length and P_s is the dissipated RF power, depends mainly on the distance between the ends of the protrusions, i.e. the effective aperture diameter $2r_a$, Fig. 1d, Fig. 2.

The structure has no rotational symmetry, which removes
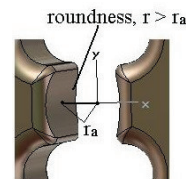
Figure 2: The structure shape near the axis for the reduction of multipole additions.

the problem of overlapping modes with perpendicular field orientation. But in the field distribution exist, together with the desirable dipole components $\sim cos(\varphi), sin(\varphi)$, multipole components $\sim cos(n\varphi), sin(n\varphi), n = 3, 5, 7, ..,$

which provide non linear additions $\sim r^{(n-1)}$ in the deflecting field. The relative amount of multipole additions can be effectively reduced by a special shape of the ends of the protrusions, Fig. 2. The roundness radius $r > r_a$, Fig. 2 should be optimized for the chosen value of r_a thus compromising the linearity of the field in the specified vicinity of the axis $r < r_0$ and the RF efficiency Z_e.

TW OPERATION

For a constant impedance structure the deflecting voltage V_d, the attenuation constant α and the normalized deflecting field $\frac{E_d^0 \lambda}{\sqrt{P_t}}$ relate as:

$$V_d = \frac{E_d^0}{\alpha}(1 - e^{-\alpha L}), \alpha = \frac{\pi}{\lambda |\beta_g| Q}, \frac{E_d^0 \lambda}{\sqrt{P_t}} = \sqrt{\frac{2\pi \lambda Z_e}{|\beta_g| Q}}, \tag{3}$$

where P_t is the input RF power and Q is the quality factor of the structure.
In Fig. 3 the calculated surfaces $\beta_g(r_a, \theta_0)$ and $Z_e(r_a, \theta_0)$ for aperture radii $0.06 \leq \frac{r_a}{\lambda} \leq 0.15$ and phase advance $20^o \leq \theta_0 \leq 179^o$ are shown for a TW operation. As can be seen from Fig. 3b, high values of $Z_e \sim 70MOm/m$ can be realized for $60^o \leq \theta_0 \leq 140^o$ and $\frac{r_a}{\lambda} \sim 0.07$. For $\frac{r_a}{\lambda} \sim 0.15$ both TE deflector and DLW reach comparable shunt impedances Z_e but, as compared to a DLW, the considered structure is not restricted in β_g, Fig.3a.
For each phase advance θ_0 the structure has an inversion
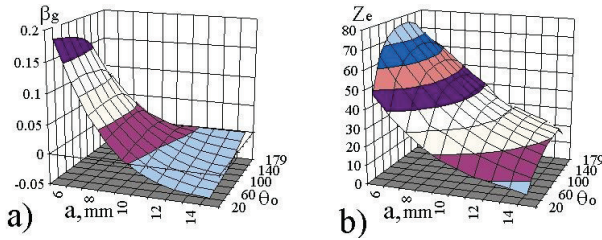
Figure 3: The surfaces of $\beta_g(r_a, \theta_0)$ (a) and $Z_e(r_a, \theta_0)$ for the TE-structure, $\lambda = 10cm$.

point at $r_a = r_{ai}$, where $\beta_g = 0$, as can be seen from Fig. 3a. The dependence $r_{ai}(\theta_0)$ is plotted in Fig. 4a as brown curve. The inversion point corresponds to the condition $H_y^0 = 0$, i.e. zero amplitude of the synchronous spatial harmonics in the transverse H_y component. In this report we consider the structure parameters for $r_a < r_{ai}$, assuming HE - domination. For $r_a > r_{ai}$ the components E_x and H_y have an opposite phasing. It is accompanied by a shunt impedance reduction, Fig. 3b.
For typical values of $\beta_g = 0.01, 0.02$ the dependencies of r_a, α and $\frac{E_d^0 \lambda}{\sqrt{P_t}}$ on θ_0 are plotted in Fig. 4. Generally, the structure has a lower Q value, as compared to a DLW, especially for $\theta_0 < 60^o$ and the attenuation constant α for this region is rather high. But, in combination with the large value of $\frac{E_d^0 \lambda}{\sqrt{P_t}}$ the structure reaches due to the higher Z_e a higher total deflecting voltage V_d. The deflecting field

03 Technology

3B Room Temperature RF
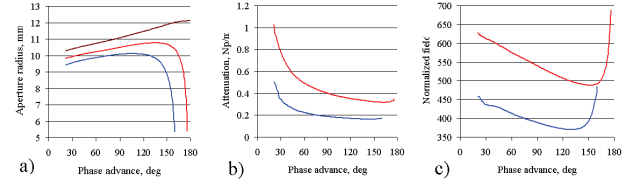
Figure 4: The dependencies of aperture radius r_a (a), attenuation α (b) and normalized field $\frac{E_d^0 \lambda}{\sqrt{P_t}}$ (c) on θ_0 for $\beta_g = 0.01$ (red) and $\beta_g = 0.02$ (blue).

distributions for the TW mode are not considered in this report.

SW OPERATION

As can be seen from Fig. 3b, for SW operation, i.e. $\theta = 180^o$, the shunt impedance Z_e reaches not the maximal value. If an aperture radius r_a is specified, two parameters can be used to tune the operating frequency - the cell radius r_c and the window radius r_w, Fig.1. In Fig. 5 the dependence of Z_e on the aperture radius r_a is plotted for a fixed window radius r_w.
For small aperture radii the operating passband of the
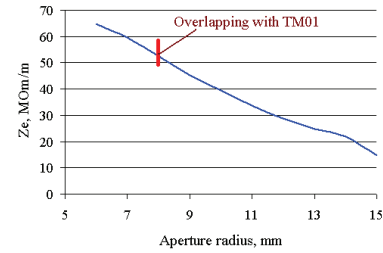
Figure 5: Z_e dependence on the aperture radius for $\theta_0 = 180^o, r_w = const$.

TE_{11}-like mode is the lowest band and the nearest TM_{01} passband is $\approx 500MHz$ higher. With increasing aperture the cell radius r_c increases too and the TM_{01} passband moves down. Due to the thick disk of approximately half a period length, modes of other types, except the operating mode, have a very weak coupling and a very narrow passband width of ($\sim 10MHz$). The vertical red line in Fig. 5 marks the range of r_a where the TM_{01} passband is closer to the operating frequency than $\pm 30MHz$.
Changing the window radius r_w both the operating frequency and the balance $\frac{Z_0 H_y^0}{E_x^0}$ in the deflecting field distribution are modified. A reduction of r_w simultaneously reduces both Z_e, and $\frac{Z_0 H_y^0}{E_x^0}$. The relative reduction of H_y^0 leads to a reduction of the operating passband width, which is just $\sim 16MHz$ for $H_y^0 = 0$. In Fig. 6 examples of deflecting field distribution are shown for different balance values $\frac{Z_0 H_y^0}{E_x^0}$, assuming the average deflecting field $10MV/m$. The plots of the amplitudes E_d are shown in

a)   b)   c)
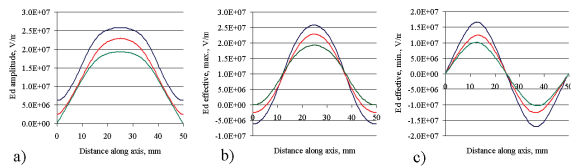
Figure 6: Distribution of the deflecting field amplitude (a), the effective field for bunch deflection (b) and bunch rotation (c) for harmonics balance $\frac{Z_0 H_y^0}{E_x^0} = 0.23$, (blue), 0.07 (red) and 0 (green) along the periodical axis.

Fig. 6a and $|E_d| \approx 0$ at the period ends for $\frac{Z_0 H_y^0}{E_x^0} = 0$. For bunch deflection the bunch center moves synchronously with the maximum of the total deflecting field, i.e. $\delta\psi = 0$. The effective deflecting field as seen by the particles is plotted in Fig. 6b. Sections with different sign of E_d can be seen, thus the deflected bunch will oscillate around the average deflected trajectory in this structure.

Today deflecting structures are widely used for another purpose, [4], related to bunch rotation. In this case the bunch center should move in a zero deflecting field, i.e. $\delta\psi = 90^o$, and the effective oscillating field becomes comparable to the amplitude of the average deflecting field, as shown in Fig. 6c. Thus together with the rotation, the bunch will oscillate as a whole along axis. Structure application for bunch rotation should hence be considered together with beam dynamics simulations. The high shunt impedance allows a higher deflecting voltage but large oscillations are not desirable from a beam dynamics point of view.

ADDITIONAL TOPICS

a)   b)
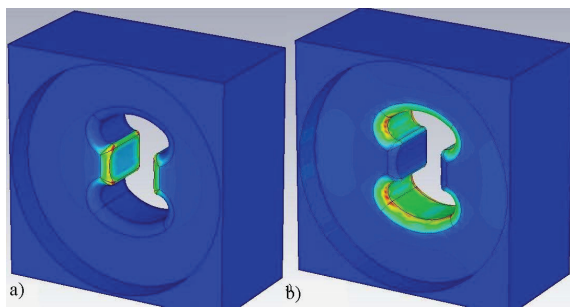
Figure 7: Electric (a) and magnetic (b) energy density distributions at the structure surface.

The somewhat more complicated structure shape, as compared to a DLW, presents no problem for modern numerically controlled tools. For the tuning after brazing the structure has an additional possibility: The distributions of the electric and magnetic energy densities at the structure surface are shown in Fig. 7 and a clear spatial separation can be seen. Four blind holes can be manufactured into the thick disk close to vicinity of the axis. After brazing of the structure small surface deformations in opposite holes, provide both positive and negative shift of the operating

frequency.

With three independent parameters, $r_a < r_w < r_c$, the structure can be modified essentially. For $r_w \to r_a$ the structure transfers into the well studied DLW. Results for the opposite direction $r_w \to r_c$ are shown in Fig. 8.

The structure diameter becomes smaller, $2r_c \leq \lambda/2$ and
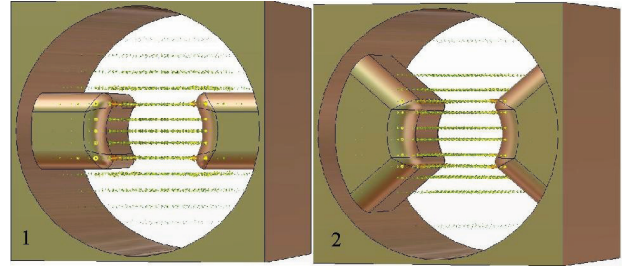
Figure 8: The structure modifications for $r_w = r_c$.

low frequency operation is possible. From an RF point of view the field distribution, can be considered either as for two transverse coaxial protrusions with opposite phasing or similar to a TM_{010} pillbox cavity with axis in x direction. For particle deflection along z-axis the structure remains HE_1 - dominated, with $\frac{Z_0 H_y^0}{E_x^0} \sim 0.4$, i.e. with stronger oscillations of the deflecting field, as shown in Fig. 6.

For manipulations of heavy ion beams, $\beta \ll 1$, [5], the magnetic component in the deflecting field (2) is negligible and the ions will see only the E_x component, similar to the case $\frac{z_0 H_y^0}{E_x^0} = 0$ in Fig. 6.

SUMMARY

RF parameters of a TE -type deflector are considered for the S - band frequency range. A higher shunt impedance, as compared to a classical DLW, can be obtained, leading to a higher deflecting voltage. Some methodical topics are considered too.

REFERENCES

[1] V. Paramonov, L. Kravchuk, S. Korepanov. Effective Standing Wave RF Structure for Particle Beam Deflector. Proc. 2006 LINAC Conf., p. 649

[2] V. Paramonov. Particularities of normal conducting L-band deflecting cavities. http://indico.cern.ch/conferenceDisplay.py?confId=83532

[3] H. Hahn, Deflecting Mode in Circular Iris-Loaded Waveguides, Rev. Sci. Inst., v. 34, n. 10, p. 1094, 1963

[4] R. Akre et. al., A Transverse RF Deflecting Structure for Bunch Length and Phase Space Diagnostic. Proc. 2001 PAC, p. 2353

[5] S. Minaev et.al., Electro-Dynamics Characteristics of RF Wobbler Cell for Heavy Ion Beam. Proc. 2010 LINAC Conf., p. 581